

# Characterization of Ni-Cu-based catalysts for multi-fuel steam reformer

Khzouz, M; Wood, J; Kendall, K, and Bujalski, W.

Published PDF deposited in Coventry University Repository

**Original citation:**

Khzouz, M; Wood, J; Kendall, K, and Bujalski, W. (2012) Characterization of Ni-Cu-based catalysts for multi-fuel steam reformer. *International Journal of Low-Carbon Technologies* 7 (1), 55-59. DOI: 10.1093/ijlct/ctr019

<http://dx.doi.org/10.1093/ijlct/ctr019>

Oxford University Press

**Copyright © and Moral Rights are retained by the author(s) and/ or other copyright owners. A copy can be downloaded for personal non-commercial research or study, without prior permission or charge. This item cannot be reproduced or quoted extensively from without first obtaining permission in writing from the copyright holder(s). The content must not be changed in any way or sold commercially in any format or medium without the formal permission of the copyright holders.**

# Characterization of Ni–Cu-based catalysts for multi-fuel steam reformer

Martin Khzouz<sup>1\*</sup>, Joe Wood<sup>2</sup>, Kevin Kendall<sup>1</sup> and Waldemar Bujalski<sup>1</sup>

<sup>1</sup>Centre for Hydrogen and Fuel Cell Research, School of Chemical Engineering, The University of Birmingham, Edgbaston B15 2TT, UK; <sup>2</sup>Catalysts and Reactions Group, School of Chemical Engineering, The University of Birmingham, Edgbaston B15 2TT, UK

## Abstract

Low-temperature methane and methanol steam-reforming catalysts Ni/Al<sub>2</sub>O<sub>3</sub>, Cu/Al<sub>2</sub>O<sub>3</sub> and Ni–Cu/Al<sub>2</sub>O<sub>3</sub> with various loadings of Ni and Cu were prepared using a wet impregnation method. The samples were characterized using scanning electron microscope, surface area (BET) test, X-ray diffraction (XRD), infrared test, CO chemisorption test and temperature-programmed reduction tests. XRD testing showed that NiO and CuO were present. Ni–Cu-alloyed catalyst shows a significant change in the catalyst characteristics compared with those of individual metals. The results presented in this paper show the main changes in the catalyst properties using *ex situ* testing.

**Keywords:** hydrogen; methane steam reforming; methanol steam reforming; fuel reformer; Ni–Cu catalyst

\*Corresponding author:  
mnk932@bham.ac.uk; www.fuelcells.bham.ac.uk

Received 31 May 2011; accepted 14 July 2011

## 1 INTRODUCTION

After the oil crises in the 1970s, the employment of hydrogen as an energy vector increased rapidly. Hydrogen is commercially produced for chemical industry for use as an intermediate reactant in methanol and ammonia production. It is also employed in hydrogenation of crude oil and hydrocracking process in steel production. However, fuel cell technology developments over the past 10 years have increased the interest in hydrogen for low-carbon technology in mobile and stationary applications [1]. Hydrogen will offer a crucial solution for transportation sectors as well as stationary applications when fuel cell technology is fully developed.

Hydrogen is likely to contribute to the energy market in the short-to-medium term in Europe [2]. However, hydrogen produced in large centralized plants requires an infrastructure network for storage, transmission and distribution. Before that infrastructure is fully established, it is convenient to produce hydrogen on-board from carrier molecules such as methane and other hydrocarbons. This can be achieved by using the fuel-processing (reforming) technology.

Fuel reforming is the conversion of hydrocarbon or other hydrogen energy carriers into pure hydrogen and carbon monoxide or carbon dioxide [3]. Methanol, natural gas, gasoline, diesel and ethanol are fuels that can be employed as the fuel for such process. Steam reforming, partial oxidation and

auto-thermal reforming are the three methods of fuel-reforming process for on-board hydrogen production.

The design of the fuel reformer depends on several factors such as the temperature required for fuel reforming, the level of by-products that connected system can tolerate, the daily cycle of the reformer and the fuel used to produce hydrogen. High efficiency, compact, fast start up, rapid responses and low cost of fuel reformer are challenges that can be solved essentially by catalyst development [4].

Heterogeneous catalysts are used because the reactants are generally in the gas phase and can be readily passed through a solid catalyst bed [5]. These catalysts, given in Table 1, can be divided into three categories: oxide catalysts, noble metal catalysts and base metal catalysts [6]. Each type of catalyst has its unique properties that can be distinguished during the reforming process via the catalyst performance criteria (conversion, yield, selectivity and activity of catalyst).

In this study, various loadings of Ni<sub>x</sub>–Cu<sub>y</sub> supported on Al<sub>2</sub>O<sub>3</sub> are characterized in order to develop a new catalyst for low-temperature methane and methanol steam reforming. Ni–Cu catalysts have been previously used for ethanol steam reforming [7–10], methane decomposition [11–13], methane partial oxidation [14] and methanol steam reactions [7]. In the present study, we investigate Ni–Cu catalysts in order to use them for methane and methanol steam reactions to develop a multi-fuel reformer catalyst.

## 2 EXPERIMENTAL METHODS

### 2.1 Catalyst preparation

$\text{Ni}_x\text{-Cu}_y/\text{Al}_2\text{O}_3$  catalysts ( $x = 10, 7, 5, 3$  and  $0\%$  weight and  $y = 0, 3, 5, 7$  and  $10\%$ , respectively) were prepared using an impregnation method. Briefly, nickel nitrate ( $\text{Ni}(\text{NO}_3)_2 \cdot 6\text{H}_2\text{O}$ ) and copper nitrate ( $\text{Cu}(\text{NO}_3)_2 \cdot 3\text{H}_2\text{O}$ ) (Fisher Scientific) were dissolved in ethanol. The metal solution was mixed using a magnetic stirrer for 30 min and then 6 g of tribole  $\text{Al}_2\text{O}_3$  (Johnson Matthey) were added to the solution and was further mixed for 2 h using a sound wave mixer at  $27^\circ\text{C}$ . Then, the prepared catalysts were dried overnight using a static oven at

$100^\circ\text{C}$ . Finally, the catalyst was calcined in oven at  $500^\circ\text{C}$  in air for 5 h at heating and cooling rates of  $5^\circ\text{C}/\text{min}$ .

### 2.2 Characterization

The samples were characterized using scanning electron microscope (SEM), surface area (BET) test, X-ray diffraction (XRD), infrared test (IR), CO chemisorption test and temperature-programmed reduction (TPR) tests.

SEM (Philips XL-30) of the sample was performed after coating with Au. BET surface area measurements were made using a Micrometrics ASAP 2010 analyser. 1.4 g of the sample was measured by plotting  $\text{N}_2$  physisorption isotherms at  $-196^\circ\text{C}$ .

XRD of the samples was performed using a Philips diffractometer. The data were sampled at  $0.02^\circ$  in the two theta range from  $5^\circ$  to  $90^\circ$  at room temperature.

DRIFTS test or IR test for catalysts was performed using a Bruker Tensor 37. The catalyst was crushed and sieved with KBr and absorption spectra were monitored in the high-frequency and low-frequency regions.

CO chemisorption tests were performed using a Micrometrics AutoChem 2920 analyzer. The temperature was increased to  $450^\circ\text{C}$  with carrier gas  $10\% \text{H}_2/90\% \text{Ar}$  at flow rate of  $10 \text{ ml}/\text{min}$  for pretreatment purposes. 1.15 g of crushed catalyst was reduced at temperature  $450^\circ\text{C}$  for 2 h using  $10\% \text{H}_2/90\% \text{Ar}$  at flow rate of  $10 \text{ ml}/\text{min}$ . Helium flow rate of  $10 \text{ ml}/\text{min}$  was introduced after reduction followed by cooling the sample to ambient temperature. Finally, CO adsorption test was investigated at temperature  $30^\circ\text{C}$  at flow rate of  $20 \text{ ml}/\text{min}$  with helium as a carrier gas at flow rate of  $50 \text{ ml}/\text{min}$ .

**Table 1.** Main advantages and disadvantages of catalysts [6].

Category	Example	Properties
Oxide catalysts	$\text{MgO}$ , $\text{Al}_2\text{O}_3$ , $\text{V}_2\text{O}_5$ , $\text{ZnO}$ , $\text{TiO}_2$ , $\text{La}_2\text{O}_3$ , $\text{CeO}_2$ , $\text{Sm}_2\text{O}_3$ , $\text{La}_2\text{O}_3\text{-Al}_2\text{O}_3$ , $\text{CeO}_2\text{-Al}_2\text{O}_3$ , $\text{MgO-Al}_2\text{O}_3$ , $\text{Al}_2\text{O}_3$ and $\text{V}_2\text{O}_5$	Normally good activity but low selectivity
Noble metal catalysts	Rh, Ru, Pt and Pd	Active, high selectivity but the cost is high
Base metal catalysts	Co based ( $\text{Co}/\text{ZnO}$ ), Cu based and Ni based ( $\text{Ni}/\text{Al}_2\text{O}_3$ )	Co based: good catalytic performance, but rapidly deactivate Cu based: good activity at low reaction temperature, while $\text{H}_2$ selectivity is poor Ni based: high conversion and the $\text{H}_2$ selectivity, but may occur coke deposition and a severe deactivation

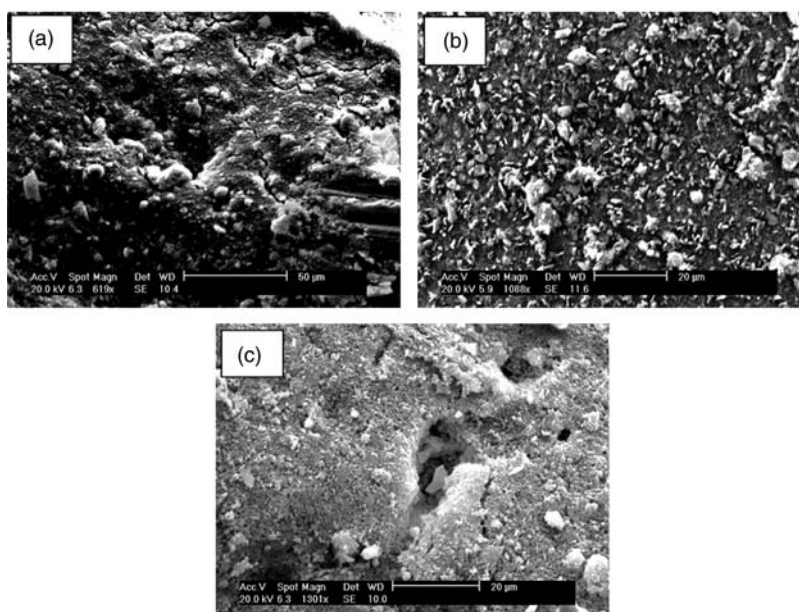


**Figure 1.** SEM of (a) 10%  $\text{Ni}/\text{Al}_2\text{O}_3$ ; (b) 10%  $\text{Cu}/\text{Al}_2\text{O}_3$  and (c) 5%  $\text{Ni}$ -5%  $\text{Cu}/\text{Al}_2\text{O}_3$ .

TPR experiments were conducted on 1 g of sample. 10% H<sub>2</sub> in argon was introduced at 500°C for 1 h then the sample was cooled to ambient temperature. 10% H<sub>2</sub> was introduced again for 30 min until the flow was stabilized. After that, the temperature was increased to 900°C at 10°C/min to monitor hydrogen uptake using a thermal conductivity detector.

## 3 RESULTS AND DISCUSSION

### 3.1 SEM test

Figure 1 shows SEM analysis for three types of prepared catalysts. It can be seen from this figure that the Ni particles are distributed uniformly on the Al<sub>2</sub>O<sub>3</sub> surface with some particles aggregated. Figure 1b indicates that the Cu particles might

remain outward of Al<sub>2</sub>O<sub>3</sub> surface with uniform distribution. Figure 1c shows that Ni and Cu particles are distributed around the pores of the support. This might indicate that Ni–Cu particles distribute more efficiently than pure metal catalysts.

### 3.2 BET test

Table 2 summarizes the BET surface area and pore volume of various formulations of the catalysts used. High metal loading (10%) showed the lowest surface area and pore volume. Pure Ni catalysts showed high surface area compared with Cu catalysts. It was interesting to see that Ni–Cu compositions revealed higher surface area compared with the pure metal catalyst at equal metal loadings.

### 3.3 XRD test

XRD patterns of the samples (Figure 2) show the characteristic peaks of NiO and CuO. The support patterns show the presence of  $\gamma$ -Al<sub>2</sub>O<sub>3</sub> and  $\theta$ -Al<sub>2</sub>O<sub>3</sub>. Other metal phases related to Ni and Cu was not identified at this stage of the test. Applying Scherrer's equation ( $t = 0.9\lambda / (B \cos \theta)$ ) to the metal oxides showed that the average particle diameter of NiO was 24.4 nm and CuO was 31.3 nm. Studying the XRD patterns of 5% Ni–5% Cu/Al<sub>2</sub>O<sub>3</sub> indicated the formation of Ni<sub>x</sub>Cu<sub>1-x</sub>O. There is a shift in peaks compared with pure metal catalyst which could be related to Cu particles size. The average particle crystallite diameter was 19.3 nm.

### 3.4 IR test

IR spectra for prepared catalysts showed high-frequency region with bands at 3440/cm and low-frequency region with bands at

Table 2. Results of BET for calcined samples at 500°C for 5 h.

Sample	BET surface area (m <sup>2</sup> /g)	Pore volume (ml/g)
10% Ni	122	0.61
10% Cu	120	0.63
7% Ni	144	0.67
7% Cu	131	0.66
5% Ni	146	0.68
5% Cu	130	0.65
3% Ni	146	0.70
3% CU	143	0.71
7% Ni–3% Cu	125	0.62
5% Ni–5% Cu	128	0.63
3% Ni–7% Cu	125	0.63

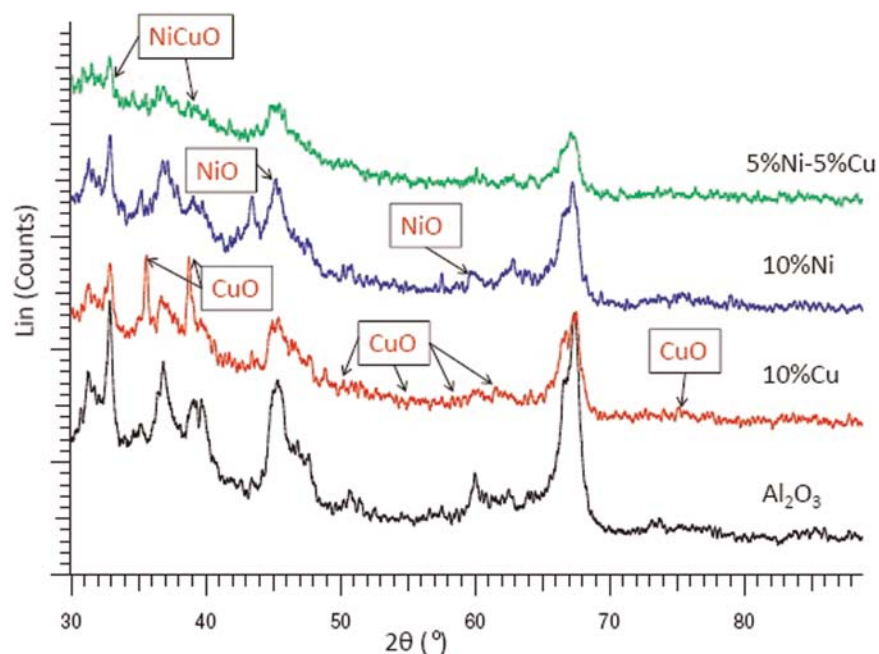


Figure 2. XRD diffraction of (a) 10% Ni/Al<sub>2</sub>O<sub>3</sub>; (b) 10% Cu/Al<sub>2</sub>O<sub>3</sub> and (c) 5% Ni–5% Cu/Al<sub>2</sub>O<sub>3</sub>.

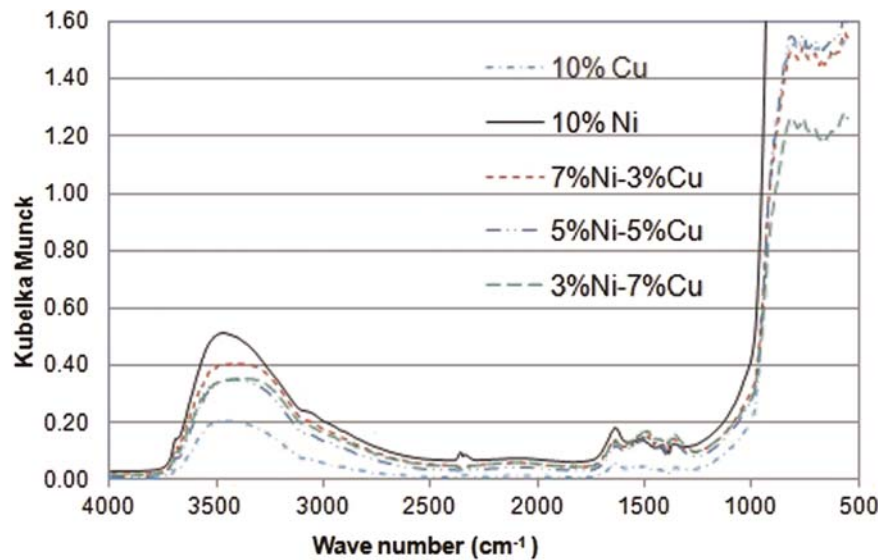


Figure 3. IR spectra for various catalyst loadings.

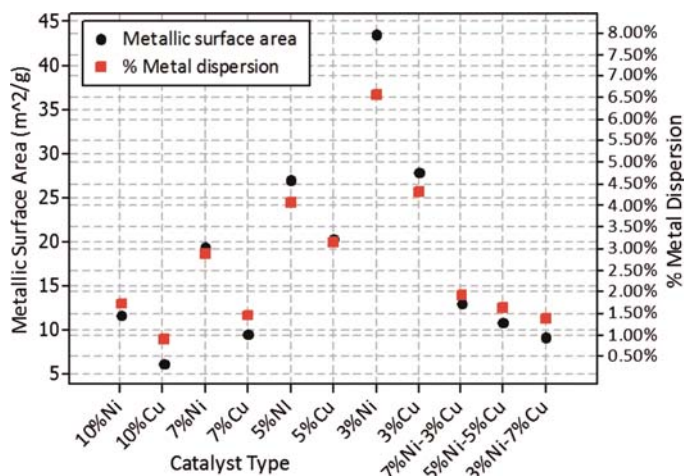


Figure 4. Metal surface area and metal dispersion for various catalyst loadings.

1520/cm as illustrated in Figure 3. At low frequency, Ni–Cu catalysts showed three active peaks which can be related to pure Ni and Cu metal particles plus an alloy of Ni–Cu particles.

### 3.5 CO chemisorptions

The CO chemisorption experiment revealed that Ni catalysts have high metallic surface area and metal dispersion (Figure 4). Ni–Cu catalysts present higher metal surface area and metal dispersion for equal metal loadings. The particle size of Cu catalyst (Figure 5) is bigger than those of other catalyst system which shows that addition of Cu will increase the active particle size of Ni–Cu catalysts.

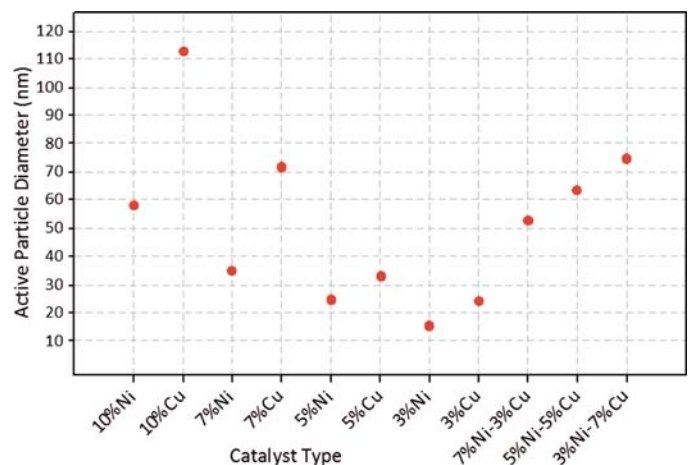


Figure 5. Active particle diameter for various catalyst loadings.

### 3.6 TPR test

Figure 6 shows the TPR spectra for three catalyst systems, pure Ni catalyst, pure Cu catalyst and Ni–Cu catalyst. Hydrogen uptake for Cu catalyst showed only one narrow peak at 165°C. Ni catalysts display a broad multi-peak at 420 and 700°C, demonstrating a range of interactions between NiO and the Al<sub>2</sub>O<sub>3</sub> support. The low reduction temperature indicates weak interaction between NiO and Al<sub>2</sub>O<sub>3</sub> while the high reduction temperature could be related to a strong interaction between NiO and Al<sub>2</sub>O<sub>3</sub> support. TPR profile of Ni–Cu catalysts shows three hydrogen uptake peaks. The first sharp peak at 180°C is associated with pure Cu catalyst but shifted compared to pure Cu catalyst system. The other two broad peaks at 390 and 620°C can be associated with Ni–Cu alloy particles and Ni metal reduction, respectively.

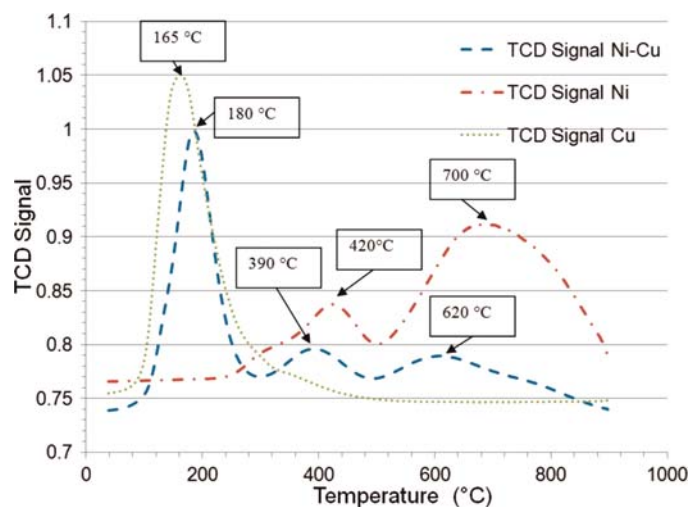


Figure 6. TPR of 10% Cu/Al<sub>2</sub>O<sub>3</sub>, 10% Ni/Al<sub>2</sub>O<sub>3</sub> and 5% Ni–5% Cu/Al<sub>2</sub>O<sub>3</sub> catalysts.

## 4 CONCLUSIONS AND FUTURE WORK

Catalyst characterizations for pure Ni, Cu and Ni–Cu catalysts supported on Al<sub>2</sub>O<sub>3</sub> for various metals loadings have been presented. The main results can be summarized:

- SEM images showed uniform distribution of Ni and Cu metals. The results indicate that Ni particles might distribute more uniformly around the pores than Cu particles. Aggregation of Ni particles was noticed.
- Ni catalysts showed higher surface area compared with Cu catalysts. On the other hand, Ni–Cu revealed higher surface area compared with the pure metal catalyst for the equal metal loadings.
- XRD testing showed that NiO and CuO were present. Formation of Ni<sub>x</sub>Cu<sub>1-x</sub>O appeared on Ni–Cu catalysts. There was a shift in Ni–Cu catalyst peaks compared with pure metal catalyst, which could be related to a change in the Cu particle size.
- Ni–Cu catalysts showed three active peaks using the IR test at low frequency, which can be related to pure Ni and Cu metal particles plus an alloy of Ni–Cu particles.
- Ni–Cu catalysts present higher metal surface area and metal dispersion for equal metal loadings and the addition of Cu increased the active particle size of Ni–Cu catalysts.
- Three hydrogen uptake peaks were obtained during the TPR test for Ni–Cu catalyst system, which can be interpreted in

terms of various metal interactions with the support and various metals present on the catalyst.

- Catalyst activity, selectivity for methanol and methane steam reforming will be studied in future under optimal operation conditions for each fuel.

## ACKNOWLEDGEMENTS

Centre for Applied Energy Research (CAER-int, Jordan) is acknowledged for the financial support.

## REFERENCES

- [1] Ball M, Wietschel M. The future of hydrogen—opportunities and challenges. *Int J Hydrogen Energy* 2009;34:615–27.
- [2] Mueller F, Tzimas E, Kaltschmitt M, et al. Techno-economic assessment of hydrogen production processes for the hydrogen economy for the short and medium term. *Int J Hydrogen Energy* 2007;32:3797–810.
- [3] Kolb G, Schürer J, Tiemann D, et al. Fuel processing in integrated micro-structured heat-exchanger reactors. *J Power Sources* 2007;171:198–204.
- [4] Ahmed S, Kumar R, Krumpelt M. Fuel processing for fuel cell power systems. *Fuel Cells Bull* 1999;2:4–7.
- [5] Richardson JT. *Principles of Catalyst Development*. Plenum Press, 1989.
- [6] Xuan J, Leung MKH, Leung DYC, et al. A review of biomass-derived fuel processors for fuel cell systems. *Renewable Sustainable Energy Rev* 2009;13:1301–13.
- [7] De Rogatis L, Montini T, Lorenzuti B, et al. NiCu/Al<sub>2</sub>O<sub>3</sub> based catalysts for hydrogen production. *Ener Environ Sci* 2008;1:501–9.
- [8] Carrero A, Calles JA, Vizcaíno AJ. Hydrogen production by ethanol steam reforming over Cu–Ni/SBA-15 supported catalysts prepared by direct synthesis and impregnation. *Appl Catal A Gen* 2007;327:82–94.
- [9] Vizcaíno AJ, Carrero A, Calles JA. Hydrogen production by ethanol steam reforming over Cu–Ni supported catalysts. *Int J Hydrogen Energy* 2007;32:1450–61.
- [10] Mariño F, Boveri M, Baronetti G, et al. Hydrogen production from steam reforming of bioethanol using Cu/Ni/K/[gamma]-Al<sub>2</sub>O<sub>3</sub> catalysts. Effect of Ni. *Int J Hydrogen Energy* 2001;26:665–8.
- [11] Echegoyen Y, Suelves I, Lázaro MJ, et al. Hydrogen production by thermocatalytic decomposition of methane over Ni–Al and Ni–Cu–Al catalysts: effect of calcination temperature. *J Power Sources* 2007;169:150–7.
- [12] Chen J, Li Y, Li Z, et al. Production of CO<sub>x</sub>-free hydrogen and nanocarbon by direct decomposition of undiluted methane on Ni–Cu–alumina catalysts. *Appl Catal A Gen* 2004;269:179–86.
- [13] Reshetenko TV, Avdeeva LB, Ismagilov ZR, et al. Carbon capacious Ni–Cu–Al<sub>2</sub>O<sub>3</sub> catalysts for high-temperature methane decomposition. *Appl Catal A Gen* 2003;47:51–63.
- [14] De Rogatis L, Montini T, Cognigni A, et al. Methane partial oxidation on NiCu-based catalysts. *Catalysis Today* 2009;145:176–85.